

All-fiberized very-large-mode-area Yb-doped fiber based high-peak-power narrow-linewidth nanosecond amplifier with tunable pulse width and repetition rate

Min Yang(杨敏), Ping-Xue Li(李平雪), Dong-Sheng Wang(王东生), Ke-Xin Yu(于可新), Xue-Yan Dong(董雪岩), Ting-Ting Wang(王婷婷), Chuan-Fei Yao(姚传飞), Wei-Xin Yang(杨卫鑫)

Citation: Chin. Phys. B . 2020, 29(11): 114206 . **doi:** 10.1088/1674-1056/abb3e9
Journal homepage: http://cpb.iphy.ac.cn; http://iopscience.iop.org/cpb

What follows is a list of articles you may be interested in

High efficiency sub-nanosecond electro-optical *Q*-switched laser operating at kilohertz repetition frequency

Xin Zhao(赵鑫), Zheng Song(宋政), Yuan-Ji Li(李渊骥), Jin-Xia Feng(冯晋霞), Kuan-Shou Zhang(张宽收)

Chin. Phys. B . 2020, 29(8): 084205 . **doi:** 10.1088/1674-1056/ab8ac4

Synthesis of new silicene structure and its energy band properties

Wei-Qi Huang(黄伟其), Shi-Rong Liu(刘世荣), Hong-Yan Peng(彭鸿雁), Xin Li(李鑫), Zhong-Mei Huang(黄忠梅)

Chin. Phys. B . 2020, 29(8): 084202 . **doi:** 10.1088/1674-1056/ab942c

2-μm mode-locked nanosecond fiber laser based on MoS_2 saturable absorber

Xiao-Fa Wang(王小发), Xiao-Ling Peng(彭晓玲), Qiu-Xia Jiang(姜秋霞), Xiao-Hui Gu(顾小辉), Jun-Hong Zhang(张俊红), Xue-Feng Mao(毛雪峰), Su-Zhen Yuan(袁素贞)

Chin. Phys. B . 2017, 26(11): 114205 . **doi:** 10.1088/1674-1056/26/11/114205

High-energy femtosecond Yb-doped all-fiber monolithic chirped-pulse amplifier at repetition rate of 1 MHz

Zhi-Guo Lv(吕志国), Hao Teng(滕浩), Li-Na Wang(王立娜), Jun-Li Wang(王军利), Zhi-Yi Wei(魏志义)

Chin. Phys. B . 2016, 25(9): 094208 . **doi:** 10.1088/1674-1056/25/9/094208

A comparison of single shot nanosecond and femtosecond polarization-resolved laser-induced breakdown spectroscopy of Al

Nakimana Agnes, Tao Hai-Yan, Hao Zuo-Qiang, Sun Chang-Kai, Gao Xun, Lin Jing-Quan

Chin. Phys. B . 2013, 22(1): 014209 . **doi:** 10.1088/1674-1056/22/1/014209

All-fiberized very-large-mode-area Yb-doped fiber based high-peak-power narrow-linewidth nanosecond amplifier with tunable pulse width and repetition rate*

Min Yang(杨敏), Ping-Xue Li(李平雪)†, Dong-Sheng Wang(王东生), Ke-Xin Yu(于可新), Xue-Yan Dong(董雪岩), Ting-Ting Wang(王婷婷), Chuan-Fei Yao(姚传飞), and Wei-Xin Yang(杨卫鑫)

Institute of Laser Engineering, Beijing University of Technology, Beijing 100124, *China*

(Received 10 April 2020; revised manuscript received 26 July 2020; accepted manuscript online 1 September 2020)

We demonstrate an all-fiberized narrow-linewidth nanosecond amplifier with high peak power, tunable pulse width, and repetition rate. A fiber-coupled narrow-linewidth laser diode operating at 1064.1 nm is employed as the seed source, which is gain-switched to generate nanosecond pulses with tunable pulse widths of 1–200 ns and tunable repetition rates of 10 Hz–100 kHz. By utilizing a very-large-mode-area Yb-doped fiber with a core diameter of 50 μm in the power amplifier, thresholds of the stimulated Brillouin scattering at different pulse widths and repetition rates are increased. The maximum average power reaches 30.8 W at the pulse width of 4 ns and a repetition rate of 100 kHz, corresponding to an optical-to-optical conversion efficiency of ∼ 55.2%. Pulse energy and peak power are calculated to be 0.2 mJ and 50 kW, respectively, which are limited by stimulated Brillouin scattering. The 3-dB spectral linewidth remains around 0.05 nm during the power scaling process. The stimulated Brillouin scattering limited output powers at different pulse widths and repetition rates are investigated. Peak power of 47.5 kW (0.19 mJ) is obtained for the 4 ns pulses at a repetition rate of 50 kHz, which is nearly the same as that of 4 ns pulses at 100 kHz. When the pulse width of the seed source is increased to 8 ns, peak powers/pulse energies are decreased to 19.6 kW/0.11 mJ and 13.3 kW/0.08 mJ at repetition rates of 50 kHz and 100 kHz, respectively.

Keywords: nanosecond, all-fiber amplifier, very-large mode area, tunable pulse width and repetition rate

PACS: 42.55.−f, 42.55.Wd, 42.65.Es **DOI:** 10.1088/1674-1056/abb3e9

1. Introduction

Nanosecond pulsed fiber lasers with advantages of good beam quality, high efficiency, compactness, and flexibility have attracted considerable research interests owing to their applications in industrial processing, medical care, and scientific researches.[1–3] In particular, narrow-linewidth nanosecond fiber lasers, especially those with high peak powers, are in great demand in fields such as nonlinear frequency conversion, high-resolution interferometry, coherent beam combination, and various kinds of lidars.[4–7] In the application of coherent lidars, the detection range depends on the spectral linewidth or coherence length of the laser source.[8,9] In the field of nonlinear frequency conversion, narrow spectral linewidth will increase the conversion efficiency, for the reason that the mismatch of phase is proportional to the spectral linewidth.[10] For coherent beam combining, narrow-linewidth nanosecond pulses have longer coherent length, which is advantageous for achieving the required optical path difference and increasing the combined efficiency.[11] In addition, narrow-linewidth nanosecond pulses with tunable pulse width and repetition rate are demanded in some areas to achieve the optimal output performance. For example, when the narrow-linewidth nanosecond pulses are applied as the pump source of a gas laser, the optimal output power of the gas laser is related to pulse width and repetition rate.[12] In some application fields such as coherent lidars, the narrow-linewidth nanosecond pulses should be power scalable to reach the desired target and thus increase the detection distance.[13] The configuration of the master oscillator power amplifier (MOPA) is usually adopted in narrow-linewidth nanosecond fiber lasers to scale the output power. However, the maximum peak power obtained from a fiberized narrow-linewidth nanosecond MOPA system is commonly limited by the nonlinearity of stimulated Brillouin scattering (SBS).[14,15] Therefore, many efforts have been made to suppress SBS and increase the output power of narrow-linewidth nanosecond fiber amplifiers.

The approaches being implemented on suppressing SBS in fiber amplifiers include utilizing large mode area (LMA) or photonic crystal fibers (PCF),[16] applying longitudinal stress or temperature gradient on the active fiber,[17] modulating the phase of seed pulses,[18] using specially-designed active fibers,[19] etc. In 2014, Su *et al.*[20] developed a narrow-linewidth nanosecond all-fiber amplifier that had been used in coherent beam combining. The seed pulses were obtained from a continuous-wave laser diode with a spectral linewidth of 20 kHz and an electro-optic modulator. A record average power of 913 W was achieved, corresponding to the peak

*Project supported by the National Natural Science Foundation of China (Grant No. 61675009) and the Beijing Natural Science Foundation Program, China, and Scientific Research Key Program of Beijing Municipal Education Commission, China (Grant No. KZ201910005006).

†Corresponding author. E-mail: pxli@bjut.edu.cn

© 2020 Chinese Physical Society and IOP Publishing Ltd

power of 28.6 kW. The SBS was suppressed effectively by reducing the pulse duration to 3 ns, which is because the short interaction time of pump pulses and Stokes pulses is insufficient for acoustic phonons with a lifetime of several nanoseconds in silica fiber to build up and thus less energy can be transferred from the pump pulses to the Stokes pulses. Ultimately, the maximum output power of the amplifier was limited by the onset of stimulated Raman scattering (SRS), since the peak power of 28.6 kW had reached the threshold of SRS. In this work, a repetition rate as high as 10 MHz was adopted to achieve high average power, resulting in limited pulse energy, and the peak power was relatively low. In 2019, Patokoski *et al.*[21] reported a tapered Yb-doped fiber amplifier, generating 0.5 mJ narrow-linewidth pulses with peak power of 4 kW at the pulse duration of 130 ns and pulse repetition frequency (PRF) of 5 MHz, which is highly desired in the application such as coherent lidar. A continuous-wave laser diode with a spectral linewidth of 5 MHz and an electro-optic modulator were adopted to provide narrow-linewidth nanosecond seed pulses. In the fiber amplifier, the SBS threshold was increased by employing a tapered active fiber. The change of core size resulted in a shift of the SBS gain peak, and therefore broadened the linewidth of the SBS gain spectrum. Besides, the Stokes pulses were suppressed when traveling back towards the smaller core in the tapered fiber. This method is effective, but the active fiber is difficult to fabricate due to the complicated tapering technique. In 2017, Cha *et al.*[22] developed a nanosecond fiber MOPA with a spectral linewidth of 70 MHz, which was devoted to the application of laser-based isotope production. By using a 55 μm-core Yb-doped PCF, the maximum pulse energy and peak power were achieved to be 0.4 mJ and 33 kW at the repetition rate of 150 kHz and pulse width of 12 ns. The PCFs exhibit the unique advantage of single-mode operation with a very large mode area, which has been utilized to suppress nonlinearities in many kinds of fiber MOPAs. However, its fusion splicing with common silica fiber is rather difficult due to the unavoidable air-holes collapse caused by heating, which destroys the guiding property and thus increases the fusion loss significantly. For this reason, the PCFs are usually free-space pumped, making the fiber MOPAs complex and losing the advantages of all-fiber format.

To preserve the excellent characteristics of all-fiber configuration, some commercial double-clad rare-earth-doped silica fibers with very large mode areas (VLMA) have been used to increase the thresholds of nonlinearities in fiber MOPAs.[23] In 2014, Fang *et al.*[24] demonstrated a nanosecond all-fiber amplifier based on a commercial 50 μm-core Yb-doped fiber. An arbitrary waveform generator was used to achieve tunable pulse repetition rates, and pulses with repetition rates of 2–10 kHz were investigated to obtain high pulse energy and peak power. The pulse energy of 2.3 mJ was obtained at a pulse duration of 3 ns and PRF of 10 kHz with a spectral linewidth of ∼7 nm, corresponding to a peak power of 697 kW. In this system, a gain-switched laser diode with the spectral linewidth of 0.134 nm was adopted as the seed source, which is the narrowest linewidth of seed pulse in a nanosecond all-fiber MOPA based on commercial 50 μm-core Yb-doped fiber ever reported to our best knowledge. High peak power and pulse energy had been obtained by utilizing this highly doped VLMA fiber to increase the thresholds of nonlinearities.

In this paper, we present a high-peak-power, pulse width and repetition rate tunable, narrow-linewidth nanosecond all-fiber MOPA based on commercial 50 μm-core Yb-doped fiber, which provides a suitable laser source in application fields such as nonlinear frequency conversion and coherent lidars. The all-fiber MOPA is composed of a 1064.1 nm gain-switched laser diode with a spectral linewidth of ∼0.05 nm and cascaded fiber amplifiers. The pulse width of the narrow-linewidth laser diode can be tuned from 1 ns to 200 ns at a tunable repetition rate of 10 Hz–100 kHz. Pulse widths of 4 ns and 8 ns at repetition rates of 50 kHz and 100 kHz are chosen to investigate the SBS thresholds of the fiber amplifier. A VLMA Yb-doped fiber with a core diameter of 50 μm is adopted in the main amplifier, generating pulses with the maximum average power of 30.8 W at 4 ns and 100 kHz, corresponding to an optical-to-optical conversion efficiency of 55.2%. The 3-dB spectral linewidth is maintained to be around 0.05 nm during the amplification process. To the best of our knowledge, this is the narrowest spectral linewidth obtained from a commercial 50 μm-core-diameter Yb-doped fiber of a nanosecond all-fiber amplifier with tunable pulse width and repetition rate. Output powers of the all-fiber MOPA at different pulse widths and repetition rates are all limited by the SBS. When seeded by 8 ns pulses, the pulse energies and peak powers of the all-fiber MOPA are achieved to be 0.11 mJ/19.6 kW at 50 kHz and 0.08 mJ/13.3 kW at 100 kHz. When seeded by 4 ns pulses, the pulse energies and peak powers reach to 0.19 mJ/47.5 kW at 50 kHz and 0.2 mJ/50 kW at 100 kHz.

2. Experimental setup

A schematic diagram of the narrow-linewidth nanosecond all-fiber amplifier is depicted in Fig. 1. The whole system is composed of three parts: a seed source, three pre-amplifiers, and the main amplifier. A single-mode fiber-pigtailed laser diode driven by electric pulses is adopted as the pulse seed, operating at the wavelength of 1064.1 nm with 3-dB linewidth less than 0.05 nm. The pulse durations are tunable from 1 ns to 200 ns, and are set to 4 ns and 8 ns in the following experiments. The repetition rates of the laser diode can be tuned from 10 Hz to 100 kHz, which are set to 50 kHz and 100 kHz. The output average power of the seed diode is at the μW level,

which will result in strong amplified spontaneous emission (ASE) in the following amplifiers. Therefore, two single-mode fiber amplifiers are built to increase the average power of the narrow-linewidth nanosecond pulses. The active fibers in these two amplifiers are single-mode Yb-doped fibers with a length of 0.75 m and an absorption coefficient of 250 dB/m, which are core-pumped by 976 nm single-mode fibercoupled laser diodes by wavelength division multiplexers (WDM). Band-pass filters (BPF) centered at 1064 nm with a bandwidth of 2.6 nm are inserted to filter out the ASE, and then a 0.3 nm fiber Bragg grating (FBG) with reflectivity larger than 99% combined with a fiber circulator is utilized to further eliminate the in-band ASE around 1064 nm as much as possible. To monitor the pulse stability of the seed source in realtime, a 90 : 10 optical coupler is inserted after port 3 of the fiber circulator, and a single-mode fiber isolator is used to block the backward propagating light. Finally, the average power of the seed pulses is amplified to ∼0.1 mW at a pulse width of 4 ns and a repetition rate of 100 kHz.

The seed pulses are subsequently injected into three pre-amplifiers for power scaling, in which 976 nm multi-mode fiber-pigtailed laser diodes are adopted as pump sources. The active fiber utilized in pre-amplifier 1 is 10/130 μm Yb-doped double-cladding fiber with a length of 1 m, and the absorption coefficient at 976 nm is ∼4.1 dB/m. A 1.5 m long 15/130 μm Yb-doped double-clad fiber with an absorption coefficient of 5.4 dB/m at 976 nm is employed in the pre-amplifier 2. Both the signal pulses and the pump light are coupled into the active fibers by $(2+1)\times 1$ combiners in pre-amplifier 1 and pre-amplifier 2. Then the amplified pulses are launched into pre-amplifier 3, in which a 30 μm-core Yb-doped fiber with a length of 1 m and an absorption coefficient of ∼9 dB/m at 976 nm is adopted as the active fiber. The signal pulses and pump light are coupled into the gain fiber through a $(6+1)\times 1$ combiner. The isolator in each preamplifier is employed to block the reflected light. After these three pre-amplifiers, the average power grows to 2.1 W for pulses with 4 ns pulse duration and 100 kHz repetition rate.

The amplified pulses are then injected into the main amplifier, which adopts a 50 μm-core Yb-doped double-clad fiber with an octagonal inner-clad and a diameter of 400 μm. The absorption coefficient of the active fiber at 976 nm is ∼5 dB/m, and the length of 2 m is chosen to provide enough gain as well as suppress nonlinear effects such as the SBS. The active fiber is clad pumped by two multimode fiber-coupled 976 nm LDs through a $(6+1)\times 1$ combiner. The signal fiber and output fiber of the combiner match well with the output fiber of the isolator with core/cladding diameters of 30/250 μm in the pre-amplifier and the active fiber with core/cladding diameters of 50/400 μm in the main amplifier. A pumped fiber of the combiner is utilized to monitor the backward propagating pulses. A 0.3 m long double-clad passive fiber with the same core and cladding diameters is spliced to the active fiber, which is angle cleaved at 11° to avoid signal feedback. A cladding mode stripper (CMS) is made at the output end of the passive fiber to dump the residual pump light and ASE by recoating the cladding with a high-index polymer. The gain fiber is coiled in the V-groove of a metal plate for heat dissipation, which is water-cooled to 9 ℃ during the experiments.

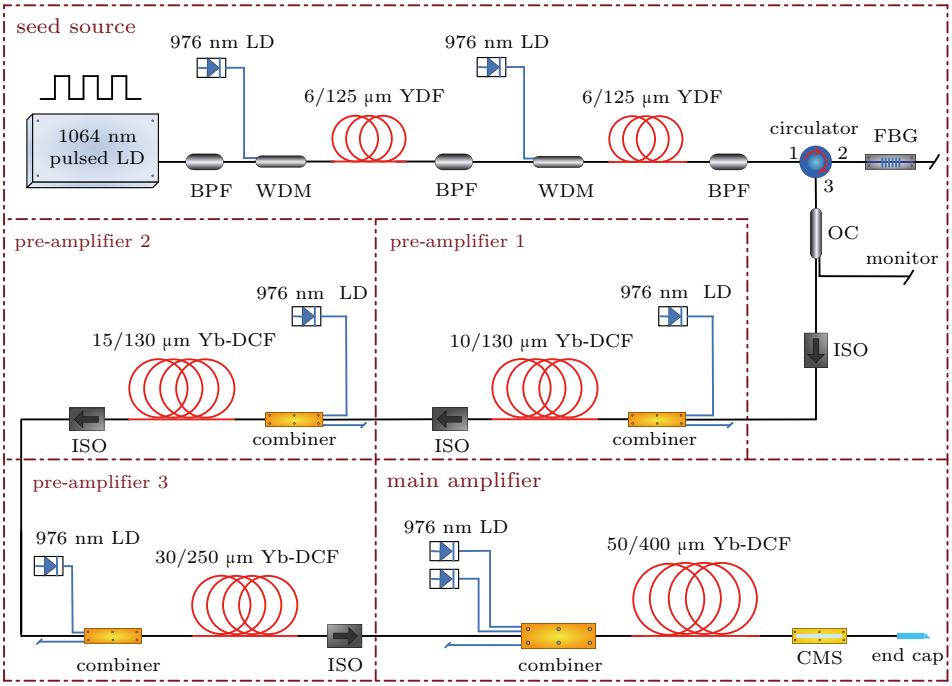


Fig. 1. Schematic diagram of the narrow-linewidth nanosecond fiber MOPA. LD, laser diode; BPF, band-pass filter; WDM, wavelength division multiplexer; YDF, Yb-doped fiber; FBG: fiber Bragg grating; OC, optical coupler; ISO, isolator; DCF, double-clad fiber; CMS, cladding mode stripper.

3. Results and discussion

When operating in continuous-wave and assuming that the pump wave is linear polarized and undepleted, the threshold of the SBS can be evaluated by[25]

$$P_{\rm cr} \approx \frac{21 \times A_{\rm eff}}{g_{\rm B} \times L_{\rm eff}}, \tag{1}$$

where $g_{\rm B}$ is the gain peak of the SBS, $A_{\rm eff}$ and $L_{\rm eff}$ are the effective mode area and effective length of the fiber, respectively. When the polarization, spectral linewidth, and gain of the pump wave are taken into account, equation (1) can be expressed as[26]

$$P_{\rm cr} \approx \frac{21 \times A_{\rm eff} \times K}{g_{\rm B} \times L_{\rm eff}} \times (1 + \Delta\nu_{\rm p}/\Delta\nu_{\rm B}) \times \ln(G), \tag{2}$$

where K is the polarization factor, G is the amplification factor of the fiber amplifier, and $\Delta\nu_{\rm p}$ and $\Delta\nu_{\rm B}$ are the spectral linewidths of the pump wave and Brillouin gain spectrum, respectively.[25–27] When operating in the pulsed regime, $L_{\rm eff}$ can be obtained from[28]

$$L_{\rm eff} \approx v_{\rm g} \times \Delta t/2, \tag{3}$$

where $v_{\rm g}$ is group velocity that can be calculated by $v_{\rm g} = c/n_{\rm g}$, $n_{\rm g}$ is the group index, and Δt is the pulse duration of the pump wave. For 1 μm pump wave in silica fiber, $g_{\rm B}$ is $\sim 3 \times 10^{-11}$ m/W and $\Delta\nu_{\rm B}$ is ~ 50 MHz.[28] When the polarization state of the pump wave is random, K is equal to 2.[26] It should be noted that equation (1) was derived based on the threshold definition that the power of Stokes wave is equal to that of the pump power at the input end of the fiber, that is,[29]

$$P_{\rm s}(0) \approx \mu P_0, \tag{4}$$

where $P_{\rm s}(0)$ is the power of Stokes wave at the input end of the fiber, P_0 is the input pump power, and the ratio $\mu = 1$. In some narrow-linewidth fiber amplifiers, $\mu = 0.01$ is also used to define the SBS threshold. In the main amplifier, $\Delta\nu_{\rm p} \approx 13.2$ GHz (0.05 nm), $n_{\rm g} \approx 1.45$, $A_{\rm eff} \approx 1075\,\mu{\rm m}^2$, and pulse durations are set to be 4 ns and 8 ns. The SBS thresholds of the main amplifier at different pulse widths and repetition rates can be calculated according to equation (2), which will be multiplied by a factor of $\mu = 0.01$. The amplification factor G can be obtained from the tested output power of the main amplifier.

It is known that the Stokes wave propagates backward in the optical fiber, which may damages components in the pre-amplifiers. Therefore, the output spectrums, temporal features, and average powers of the backward propagating pulses, as well as those of the forward-traveling signal pulses, are monitored simultaneously when increasing the incident pump power. The backward output spectrums of the main amplifier seeded by 4 ns pulses at 100 kHz are measured with an optical spectrum analyzer (YOKOGAWA, AQ6370D) at its highest resolution of 0.02 nm, as presented in Fig. 2. It can be observed that there is a peak at 1064.1 nm when the forward output power is below 15.5 W, which is the Rayleigh scattering of the signal pulse. With the increase of forward output power, a peak at a wavelength of 1064.2 nm appears. When the forward output power exceeds 17.8 W, the peak at 1064.2 nm grows rapidly. The frequency difference of these two peaks is calculated to be 15.8 GHz, which is coincident with the Brillouin frequency shift in silica fiber at 1064 nm,[25] and thus indicating the onset of the SBS. The corresponding temporal features of backward output pulses are shown in Fig. 3. It is obvious that the pulse amplitudes become to fluctuate dramatically when operating at the forward output power of 17.8 W, corresponding to the appearance of the 1064.2 nm peak in Fig. 2 and the nonlinear increase of backward power shown in Fig. 4. The reason is that at this point, the backward propagating Stokes pulses start depleting the power of forward propagating pulses in the active fiber. Therefore, it is believed that the SBS occurs, and further scaling of the average power is ceased to ensure safe and stable operation.

The measured output average powers and backward propagating powers of the main amplifier seeded by pulses with different pulse widths and repetition rates are plotted in Fig. 4. When seeded by 4 ns pulses with the PRF of 100 kHz, the maximum average power of the main amplifier reaches 30.8 W under the incident pump power of 52 W, and the corresponding optical-to-optical conversion efficiency is 55.2%. For seed

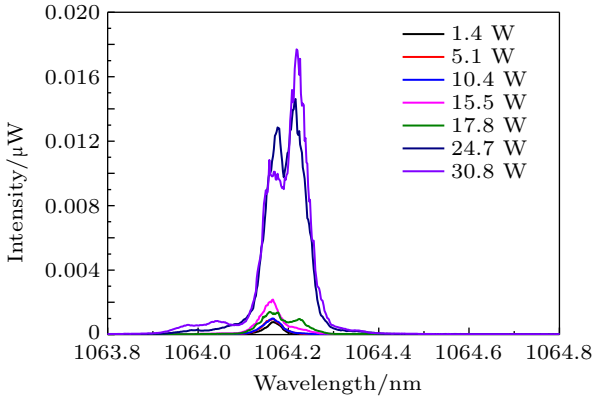


Fig. 2. Spectrum of the backward propagating pulses.

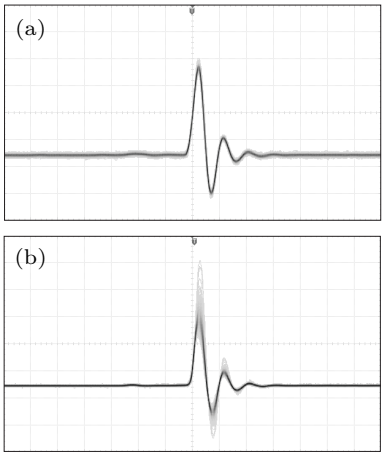


Fig. 3. Backward propagating pulses at 1.4 W (a) and 17.8 W (b).

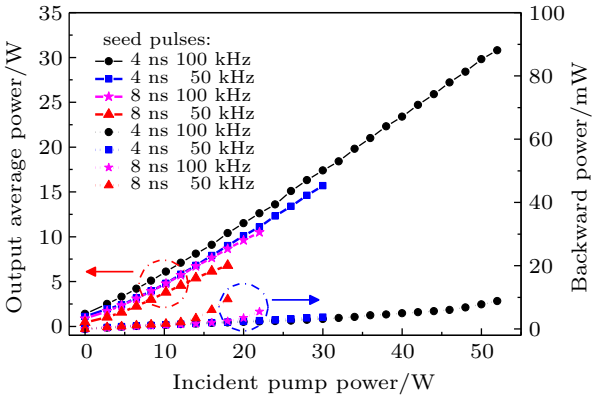


Fig. 4. Output average powers of the main amplifier at different pulse widths and repetition rates.

pulses at 4 ns and 50 kHz, the maximum average power is achieved to 15.7 W. When seeded by 8 ns pulses, the maximum average powers are 6.8 W at 50 kHz and 10.5 W at 100 kHz. The output powers grow linearly, which are all limited by the onset of the SBS, and no rollover is observed. When the pulse width is reduced from 8 ns to 4 ns, the SBS threshold is increased dramatically, which is mainly because less energy is transformed into the Stokes pulse when the pulse duration is much shorter than the acoustic phonon lifetime of several nanoseconds.[20] It is also seen that the average power increases with an increasing PRF for pulses with the same duration. This is because pulses with lower PRF can extract more energy, resulting in a higher peak power to reach the SBS threshold. Additionally, it is found that the slope efficiency is a little higher under higher PRF, which can be attributed to a higher seeding power output from the preamplifiers. The SBS thresholds at different pulse widths and repetition rates can be calculated according to Eq. (2) and the gain factors obtained from the tested output powers, which are 19.9 kW at 4 ns/50 kHz, 22.45 kW at 4 ns/100 kHz, 10.3 kW at 8 ns/50 kHz and 9.4 kW at 8 ns/100 kHz. The beam quality of the main amplifier is tested by a laser beam analyzer (M2-200, Ophir-Spiricon), shown in Fig. 5. The M^2 values of 2.561 and 3.173 are obtained in horizontal and vertical directions at the maximum average output power. It can be seen that the output beam is operating in LP_{21} mode, which could be optimized through carefully coiling the active fiber and improve the beam quality of the pre-amplifier. It is possible to achieve an LP_{01} mode according to the beam quality in Ref. [24].

The pulse temporal behaviors of the seed source and main amplifier are recorded by a photodetector (Thorlabs, PDA10CF, bandwidth: 150 MHz) and a digital oscilloscope (RIGOL, DS2202A, bandwidth: 200 MHz), as shown in Fig. 6. It can be seen from Figs. 6(a) and 6(b) that the pulse widths keep almost unchanged when the amplifier is seeded by 4 ns pulses. However, it is observed from Figs. 6(c) and 6(d) that when seeded by 8 ns pulses, the pulse widths of the main amplifier are slightly reduced to $\sim$ 5.6 ns and $\sim$ 6 ns at PRFs of 50 kHz and 100 kHz. This is due to the effect of gain saturation. The leading edge of the pulse consumes much inverted populations and experiences higher gain than the trailing edge, resulting in the narrowing of pulse duration and a steeper leading edge. When the repetition rate is reduced from 100 kHz to 50 kHz, the narrowing of pulse duration is more significant. This is because more energy has been extracted under a lower repetition rate. The insets in Figs. 6(a)–6(d) display the pulse sequences under different pulse widths and repetition rates, and the pulse-to-pulse amplitude fluctuations are less than 5%. It should be noted that ripples appear in the trailing edges of the pulses due to the slow rising time of the photodetector and oscilloscope. Therefore, photodetector and oscilloscope with larger bandwidth are required to obtain more accurate values of pulse durations.

The spectral distributions of the nanosecond pulses output from the main amplifier for the 4 ns pulses at 100 kHz are illustrated in Fig. 7. Figure 7(a) shows the output spectrum at the maximum output power of 30.8 W. We observe a pedestal with 3-dB spectral bandwidth of $\sim$ 12 nm, located at the bottom of the peak wavelength of $\sim$ 1064 nm, which is attributed to the growth of in-band ASE leaked out by the pre-amplifiers and the gain-induced broadening of the signal laser. According to the Raman frequency shift of $\sim$ 13 THz ($\sim$ 49.1 nm at 1064 nm) in silica fiber,[25] the envelope centered around 1114 nm is Stokes waves generated by the nonlinear effect of the SRS. The onset of the SRS is probably caused by the above-mentioned pedestal, which has a broad spectral bandwidth of $\sim$ 12 nm. The ASE centered around 1030 nm is observed and the signal light is larger than 40 dB above the ASE. The enlarged spectrum with a span of 2 nm is displayed in the inset of Fig. 7(a), which is measured at a resolution of 0.02 nm. The center wavelength of the pulses is 1064.165 nm, and the 3-dB spectral linewidth at the maximum output power is approximately 0.05 nm.

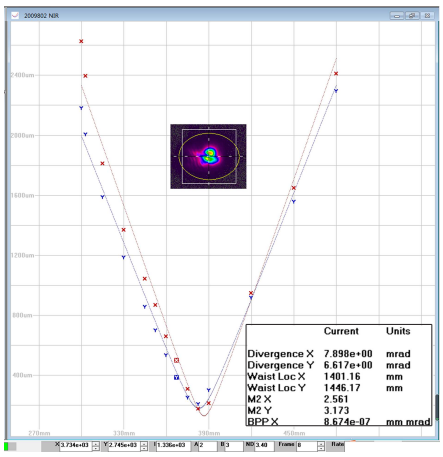


Fig. 5. The M^2 factor at the maximum output power of 30.8 W.

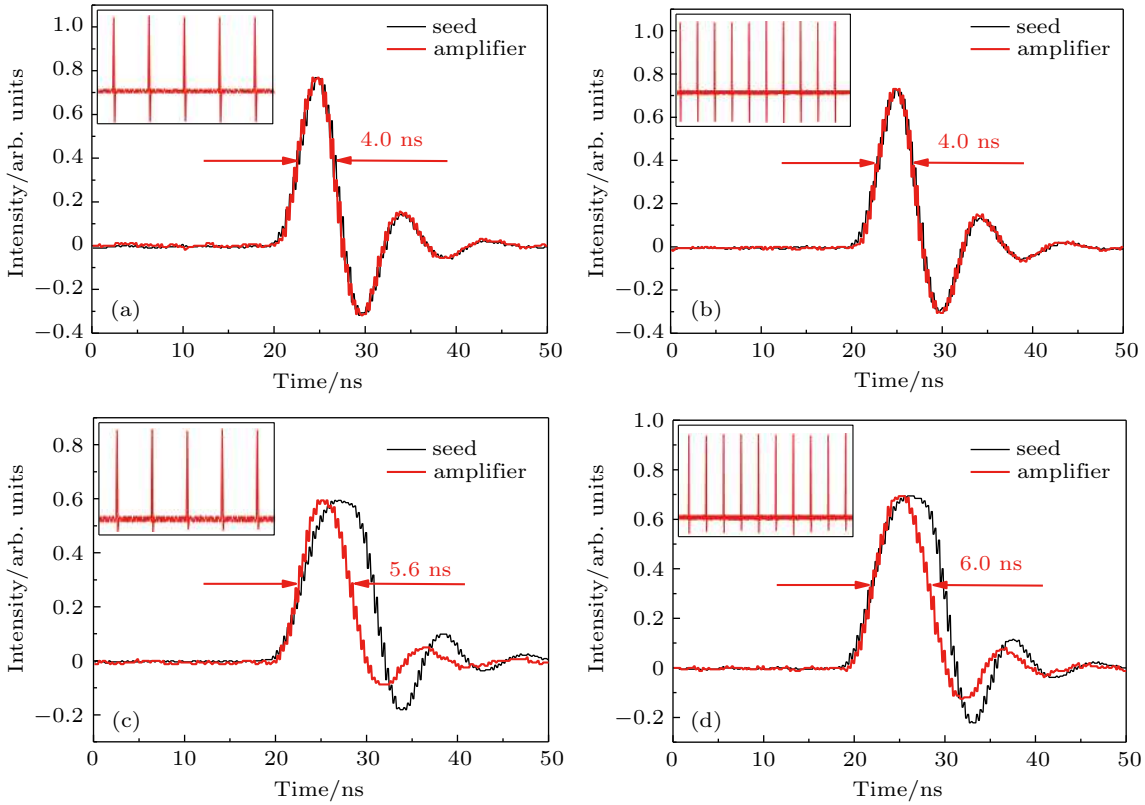


Fig. 6. Seed pulses and amplified pulses of the main amplifier seeded by pulses of 4 ns/50 kHz (a), 4 ns/100 kHz (b), 8 ns/50 kHz (c), 8 ns/100 kHz (d). Insets: pulse sequences at each pulse width and repetition rate.

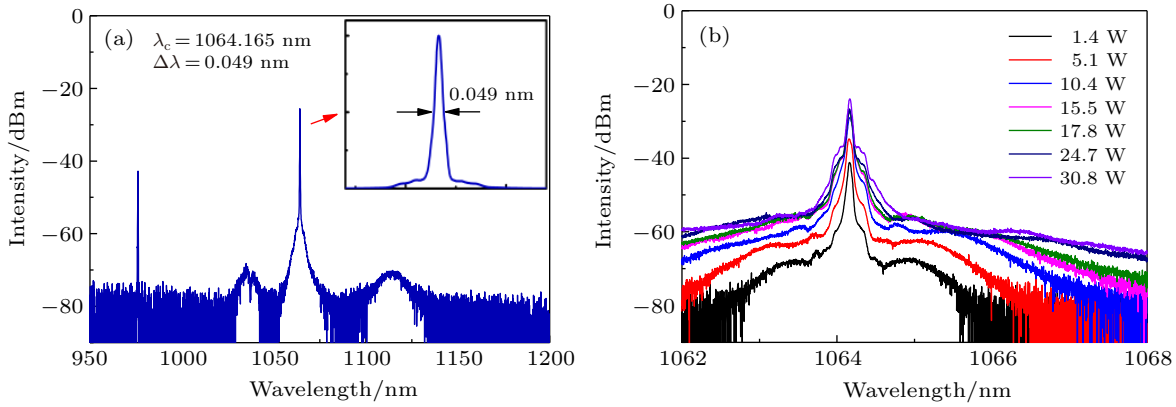


Fig. 7. Output spectrums of the main amplifier seeded by 4 ns pulses with the PRF of 100 kHz. (a) Spectral distribution at 30.8 W, inset: enlarged spectrum; (b) evolutions of spectrum.

The spectral evolutions in the main amplifier are illustrated in Fig. 7(b). There is no significant change during amplification except for the intensity of the pedestals. With the increase of output power, the optical signal-to-noise ratio gradually deteriorates. Evaluated from spectral integration, the amount of this pedestal and the residual pump light is calculated to be less than 35% of the average power at a maximum output of 30.8 W. It implies that the signal pulses account for more than 65% of the tested power. Similar features are observed in the output spectrums for pulses at 4 ns/50 kHz, 8 ns/50 kHz, and 8 ns/100 kHz. The power ratios of signal pulses are calculated in the same way, which are about 60%, 82%, and 79%, respectively.

The SBS limited peak powers of the narrow-linewidth nanosecond all-fiber amplifier are calculated from the measured average powers, pulse widths, and repetition rates, and the amount of signal pulses are taken into account according to the output spectrums as discussed above. Ultimately, the pulse energies are amplified to 0.19 mJ and 0.2 mJ for 4 ns pulses at the PRFs of 50 kHz and 100 kHz, 0.11 mJ and 0.08 mJ for 8 ns pulses at the PRFs of 50 kHz and 100 kHz. The corresponding peak powers are calculated to be 47.5 kW, 50 kW, 19.6 kW, and 13.3 kW, respectively. It can be seen that the measured SBS threshold is in good agreement with the theoretical value calculated by Eq. (2) at the pulse width of 8 and the repetition rate of 100 kHz, while the measured values are

much larger than the theoretical values at other pulse widths and repetition rates. This is probably because $\mu = 0.01$ in the definition of the SBS threshold is more accurate for 8 ns pulses at 100 kHz in the experiment, which has a tested backward power close to the pump power by a factor of 0.01. At the repetition rate of 50 kHz, the SBS threshold of 4 ns pulses is nearly 2.5 times higher than that of the 8 ns pulses, which can be explained by Eq. (3). When the repetition rate is increased to 100 kHz, the SBS threshold of 4 ns pulses is nearly 3.7 times higher than that of the 8 ns pulses, which is likely due to a larger temperature gradient along the active fiber under a higher pump power at 100 kHz. In some lidar systems, pulse parameters will influence the test resolution or signal-to-noise ratio. When applied in these conditions, different pulse parameters of this fiber MOPA could be selected accordingly. Further experiments to extend its application fields, such as increasing pulse width to hundreds of nanoseconds and lowering repetition rate to several kilohertz, are under investigation.

4. Conclusion

In summary, a narrow-linewidth nanosecond all-fiber MOPA with high peak power, tunable pulse width and repetition rate is demonstrated. Seed pulses are obtained from a 1064.1 nm gain-switched narrow-linewidth laser diode, where the pulse width is tunable in the range of 1–200 ns at a repetition rate of 10 Hz–100 kHz. By the use of a VLMA Yb-doped fiber with a core diameter of 50 μm, the SBS thresholds of the fiber amplifier at different pulse widths and repetition rates are increased. Seeded by 4 ns pulses at 100 kHz, the maximum output average power reaches to 30.8 W with an optical-to-optical conversion efficiency of 55.2%, which is limited by the SBS. The corresponding pulse energy and peak power are 0.2 mJ and 50 kW, respectively, and the spectral linewidth remains around 0.05 nm during the amplification process. The pulse energy and peak power of 4 ns pulses at 50 kHz are 0.19 mJ and 47.5 kW. When seeded by 8 ns pulses, the obtained pulse energies/peak powers are decreased to 0.11 mJ/19.6 kW at 50 kHz and 0.08 mJ/13.3 kW at 100 kHz. Further investigations to improve pulse energy and peak power of this all-fiber MOPA are anticipated by using a VLMA Yb-doped fiber with higher doping concentration, in which the SBS threshold might be effectively increased through reducing its fiber length. Besides, a solid-state amplifier can be applied to improve the pulse energy to hundreds of mJ or Joule level. Benefiting from the tunable pulse parameters and all-fiber architecture, this laser system has great potential to be applied as a laser source in fields of nonlinear frequency conversion[30] and various kinds of lidars such as Doppler wind lidars,[31] synthetic aperture lidars,[32] and 3D imaging lidars.[33]

References

[1] Niu L Q, Gao C X, He H D, Feng L, Cao Z Y, Sun C D and Zhu S L 2013 *Laser Phys.* **23** 95103
[2] Xiao Q R, Yan P, Sun J Y, Chen X, Ren H C and Gong M L 2014 *Chin. Phys. B* **23** 104221
[3] Zhang T, Zhang W G, Cai Y J, Hu X H, Feng Y, Wang Y S and Yu J 2019 *Acta Phys. Sin.* **68** 234204 (in Chinese)
[4] Su R T, Wang X L, Zhou P and Xu X J 2013 *Laser Phys. Lett.* **10** 015105
[5] Su R T, Zhang P F, Zhou P, Xiao H, Wang X L, Duan L, Lv P and Xu X J 2018 *Acta Phys. Sin.* **67** 154202 (in Chinese)
[6] Prevost F, Lombard L, Primot J, Ramirez L P, Bigot L, Bouwmans G and Hanna M 2017 *Opt. Express* **25** 9528
[7] Dolfi-Bouteyre A, Canat G, Lombard L, Valla M, Durecu A and Besson C 2017 *Opt. Eng.* **56** 31217
[8] Lombard L, Dolfi-Bouteyre A, Besson C, Augere B, Bourdon P, Durecu A, Goular D, LeGouet J, Planchat C, Renard W, Valla M and Canat G 2015 *Proc. SPIE* **9645** 96450B
[9] Feng L T, Zhao P E, Shi X D, Jin G H, Yang Z H, Zhou D F and Hou T J 2019 *Infrared Laser Eng.* **48** 0406005 (in Chinese)
[10] Ma J Q 2010 *Influence of Pump Laser Line Width in Frequency Conversion* (Master Dissertation) (Changsha: National University of Defense Technology of China) (in Chinese)
[11] Wang Y S, Ma Y, Sun Y H, Wang Y, Chang Z, Peng W J, Yang X B, Zhu R H, Zhang K and Tang C 2019 *Chin. J. Lasers* **46** 1215001 (in Chinese)
[12] Cui Y L, Tang N, Zhou Z Y, Li Z X and Wang Z F 2019 *Opt. Fiber Technol.* **52** 101938
[13] Dilley C E, Stephen M A and Savage-Leuchs M P 2007 *Opt. Express* **15** 14389
[14] Wellmann F, Steinke M, Meylahn F, Bode N, Willke B, Overmeyer L, Neumann J and Kracht D 2019 *Opt. Express* **27** 28523
[15] Wang X L, Zhou P, Leng J Y, Du W B and Xu X J 2013 *Chin. Phys. B* **22** 044205
[16] Teodoro F D, Morais J, McComb T S, Hemmat M K, Cheung E C, Weber M and Moyer R 2013 *Opt. Lett.* **38** 2162
[17] Zhu R, Wang J T, Zhou J, Liu J Q and Chen W B 2012 *Chin. Opt. Lett.* **10** 091402
[18] Ran Y, Su R T, Ma P F, Wang X L, Lv H B, Zhou P and Si L 2015 *Opt. Express* **23** 25896
[19] McComb T S, McCal D, Farrow R, Lowder T L, Logan D, Green J, Kutscha T N, Ye C G, Aallos V, Koponen J J and Fanning G 2014 *Proc. SPIE* **8961** 896112
[20] Su R T, Zhou P, Wang X L, Tao R M and Xu X J 2014 *High Power Laser Sci. Eng.* **2** e3
[21] Patokoski K, Rissanen J, Noronen T, Gumenyuk R, Chamorovskii Y, Filippov V and Toivonen J 2019 *Opt. Express* **27** 31532
[22] Cha Y H, Kim Y, Park H, Lim G, Ko K H, Kim T S and Jeong D Y 2017 *J. Korean Phys. Soc.* **70** 973
[23] Zhang H W, Wang X L, Zhou P, Gong Z Q and Xu X J 2012 *Appl. Opt.* **51** 6933
[24] Fang Q, Shi W and Fan J L 2014 *IEEE Photon. Technol. Lett.* **26** 1676
[25] Agrawal G P 2010 *Nonlinear Fiber Optics*, 4th edn & *Applications of Nonlinear Fiber Optics*, 2nd edn. (Beijing: Beijing World Publishing Corporation) p. 246 (in Chinese)
[26] Liu C, Liu J, Zhang Y J, Hou Y B, Qi S X, Feng X and Wang P 2017 *Opt. Express.* **25** 9569
[27] Huang L, Ma P F, Meng D, Li L, Tao R M, Su R T, Ma Y X and Zhou P 2018 *High Power Laser Sci. Eng.* **6** e42
[28] Smith R G 1972 *Appl. Opt.* **11** 2489
[29] Kobyakov A, Sauer M and Chowdhury D 2010 *Adv. Opt. Photon.* **2** 1
[30] Hung J H, Gao Y, Yan H J, Sato K, Yamada H, Peng L H, Nemoto T and Yokoyama H 2019 *Appl. Phys. Express.* **12** 082002
[31] Shangguan M J, Xia H Y, Wang C, Qiu J W, Shentu G L, Zhang Q, Dou X K and Pan J W 2016 *Opt. Express* **24** 19322
[32] Wang N, Wang R, Mo D, Li G Z, Zhang K S and Wu Y R 2018 *Appl. Opt.* **57** 230
[33] Lu Z Y, Zhou Y, Sun J F, Luan Z, Wang L J, Xu Q, Li G Y, Zhang G and Liu L R 2017 *Chin. J. Lasers* **44** 0110001